

Embracing C<sub>60</sub> with Multiarmed Geodesic PartnersShehadeh Mizyed,<sup>†</sup> Paris E. Georghiou,<sup>†</sup> Mihail Bancu,<sup>‡</sup> Bernardo Cuadra,<sup>‡</sup> Amarjit K. Rai,<sup>‡</sup> Peichao Cheng,<sup>‡</sup> and Lawrence T. Scott<sup>\*,‡</sup>

Contribution from the Department of Chemistry, Memorial University of Newfoundland, St. John's, Newfoundland, Canada A1B 3X7, and Department of Chemistry, Merkert Chemistry Center, Boston College, Chestnut Hill, Massachusetts 02467-3860

Received August 3, 2001. Revised Manuscript Received October 3, 2001

**Abstract:** 1,3,5,7,9-Pentakis(4-methoxyphenylthio)corannulene (**3**), 1,3,5,7,9-pentakis(2-naphthylthio)corannulene (**4**), and 1,3,6,8-tetrakis(4-methoxyphenylthio)corannulene (**5b**) have been synthesized by chlorination of corannulene with ICl in CH<sub>2</sub>Cl<sub>2</sub> at 25 °C and subsequent nucleophilic aromatic substitution with the appropriate sodium thiophenolate in DMEU at 25 °C. <sup>1</sup>H NMR titration studies demonstrate that these novel bowl-shaped hosts form 1:1 complexes with C<sub>60</sub> in toluene-d<sub>8</sub> solution with association constants of 454, 368, and 280 M<sup>-1</sup>, respectively.

## Introduction

Organic chemists learned long ago that large, planar polycyclic aromatic compounds with electron-rich faces, like those of benzene (Figure 1), form strong complexes with picric acid and other planar partners that proffer electron-deficient  $\pi$ -faces.<sup>1</sup> On the other hand, the geodesic polyarenes with curved  $\pi$ -faces that have recently become available<sup>2</sup> are geometrically ill-disposed to complex with planar partners. Indeed, corannulene (**1**) forms only a weak complex with picric acid<sup>3</sup> and with other planar, electron-deficient  $\pi$ -systems.<sup>4</sup> For optimal face-to-face contact, the partner for a geodesic polyarene such as corannulene should possess a geometrically complementary curved surface. In addition, to provide a strong intermolecular attraction, the interacting faces of the two partners should also be electronically complementary; i.e., if one surface is electron rich, the other should be electron deficient, just as in the case for two planar partners. Herein we report the first examples of complexation between derivatives of a geodesic polyarene and C<sub>60</sub>.

For planar aromatic compounds such as benzene, the two  $\pi$ -faces necessarily exhibit identical electronic character as a consequence of the molecular symmetry. For geodesic polyarenes such as corannulene, however, the electronic character of the concave and convex  $\pi$ -faces must be different. In principle, they cannot be the same. One  $\pi$ -face must be more electron rich than the other, although which face is which may not appear intuitively obvious. As we have noted before, even theoretical calculations give different answers to this question, depending on the level of theory employed.<sup>5</sup> Semiempirical

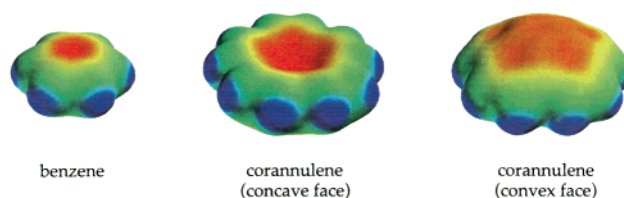


**Figure 1.** Electrostatic potential maps on the surface of benzene and corannulene (density functional theory: BP/DN\*\*). The regions of most negative electrostatic potential are shaded red, and the most positive regions are shaded blue.

calculations (AM1) predict a more negative electrostatic potential on the convex  $\pi$ -surface than on the concave  $\pi$ -surface of corannulene and of other geodesic polyarenes, whereas higher level density functional calculations (pBP/DN\*\*) predict precisely the opposite properties.<sup>6</sup> To date, there has been no experimental test of these predictions; however, the explicit inclusion of electron correlation in density functional theory probably makes the latter predictions more trustworthy (Figure 1). Regardless of which  $\pi$ -face is the more electron rich and which is the more electron deficient, of course, the two must be electronically complementary. Consequently, the face-to-face interaction of a convex  $\pi$ -surface with a concave  $\pi$ -surface will be energetically favorable.

Since the degree of curvature at the van der Waals surface on the concave  $\pi$ -face of corannulene exceeds that of the underlying polyatomic framework, the best convex guest for this geodesic polyarene should have a greater degree of curvature than corannulene in its polyatomic framework. In this respect, C<sub>60</sub> appears nearly ideal. The fact that corannulene (C<sub>20</sub>H<sub>10</sub>) forms a stable complex with (C<sub>60</sub>)<sup>+</sup> in the gas phase [(C<sub>80</sub>H<sub>10</sub>)<sup>+</sup>, *m/z* 970, eq 1] confirms that these two curved  $\pi$ -surfaces are geometrically well matched,<sup>7</sup> and solution studies with calixarenes have demonstrated that even neutral C<sub>60</sub> is sufficiently

\* To whom correspondence should be addressed. E-mail: lawrence.scott@bc.edu. Phone: 617-552-8024. Fax: 617-552-6454.

<sup>†</sup> Memorial University of Newfoundland.

<sup>‡</sup> Boston College.

(1) Review: Parini, V. P. *Russ. Chem. Rev.* **1962**, *31*, 408.

(2) (a) Mehta, G.; Rao, H. S. P. *Tetrahedron* **1998**, *54*, 13325–13370.

(b) Scott, L. T.; Bronstein, H. E.; Preda, D. V.; Ansems, R. B. M.; Bratcher, M. S.; Hagen, S. *Pure Appl. Chem.* **1999**, *71*, 209–219, and references therein.

(3) Lawton, R. G.; Barth, W. E. *J. Am. Chem. Soc.* **1971**, *93*, 1730–1745.

(4) Preda, D. V. Ph.D. Dissertation, Boston College, 2001.

(5) Klärner, F.-G.; Panitzky, J.; Preda, D.; Scott, L. T. *J. Mol. Model.* **2000**, *6*, 318–327.

(6) Molecular orbital calculations were performed using the Spartan program from Wavefunction, Inc., Irvine, CA.

(7) Becker, H.; Javahery, G.; Petrie, S.; Cheng, P. C.; Schwarz, H.; Scott, L. T.; Böhme, D. K. *J. Am. Chem. Soc.* **1993**, *115*, 11636–11637.

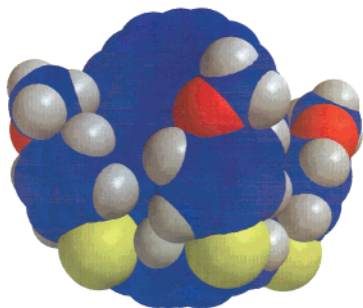
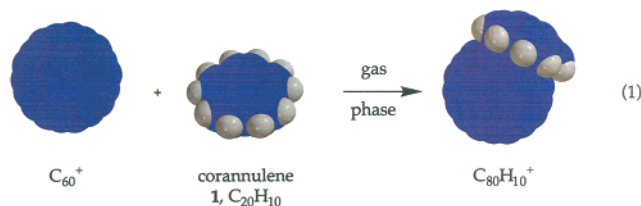


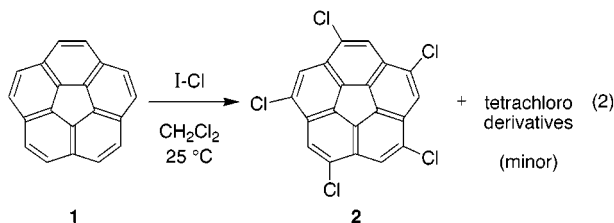
**Figure 2.** Proposed mode of complexation between C<sub>60</sub> and corannulene derivative **3** (not an X-ray structure).

electron deficient to bind to suitably constituted, “bowl-shaped” cavities that are lined with converging electron-rich surfaces.<sup>8</sup>



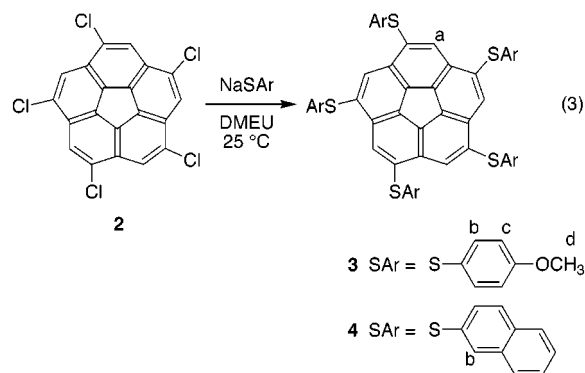
**Syntheses.** To reinforce the anticipated attraction between the concave  $\pi$ -surface of corannulene and the convex  $\pi$ -surface of C<sub>60</sub>, we prepared several corannulene derivatives bearing electron-rich arms capable of embracing the fullerene (Figure 2). The high solubility of C<sub>60</sub> in anisole (5.6 mg/mL) and in chloronaphthalene (51 mg/mL) relative to that in benzene (1.7 mg/mL) guided our choice of side chains.<sup>9</sup>

Initial functionalization of the corannulene perimeter was accomplished by chlorination with ICl in CH<sub>2</sub>Cl<sub>2</sub> at 25 °C, which gave 1,3,5,7,9-pentachlorocorannulene (**2**) as the major product (eq 2). We first discovered this surprisingly selective chlorination many years ago,<sup>10</sup> and others have since used it,<sup>11</sup> but the origin of its high selectivity remains obscure.

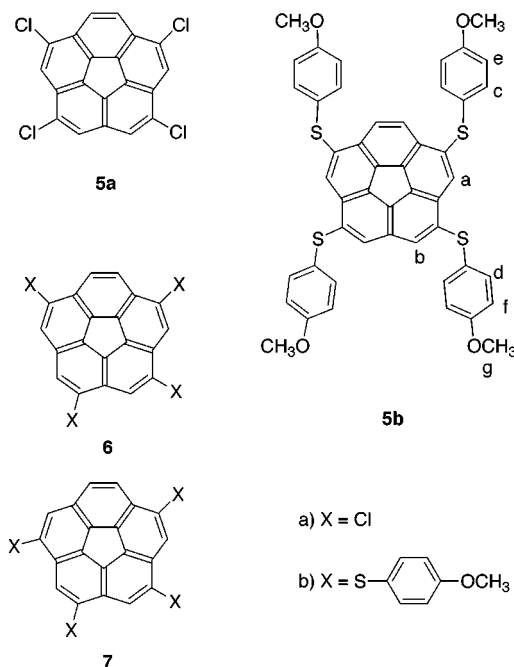


Many polyfluoro- and polychloroaromatic hydrocarbons are known to undergo nucleophilic aromatic substitution reactions with thiolates in polar aprotic solvents,<sup>12</sup> and 1,3,5,7,9-pentachlorocorannulene (**2**) also reacts in this manner.<sup>10</sup> Thus, treatment of **2** with sodium 4-methoxyphenylthiolate in DMEU at 25 °C gives 1,3,5,7,9-pentakis(4-methoxyphenylthio)corannulene (**3**), and the corresponding 1,3,5,7,9-pentakis(2-naphthylthio)corannulene (**4**) is easily prepared by the same method (eq 3). Decakis(4-methoxyphenylthio)corannulene was likewise

synthesized from perchlorocorannulene,<sup>13,14</sup> but this more highly congested derivative showed no evidence by NMR spectroscopy for complexation with C<sub>60</sub>.



When the synthesis of **3** was run on a relatively large scale and the crude product was carefully chromatographed, three tetrakis(4-methoxyphenylthio)corannulene isomers (**5b–7b**) were obtained as minor byproducts, in addition to **3**. Presumably, these tetrasulfides are all derived from small amounts of the corresponding tetrachlorocorannulenes (**5a–7a**) carried through as contaminants from the chlorination reaction (eq 2). The structures of isomers **6b** and **7b** were tentatively assigned on the basis of their <sup>1</sup>H NMR spectra, but only the C<sub>s</sub>-symmetric tetrakis(4-methoxyphenylthio)corannulene **5b** was fully characterized and used for complexation studies with C<sub>60</sub>. A (+)-mesomeric effect from the sulfur atoms is expected to release electron density into the benzene rings, thereby enhancing the  $\pi$ - $\pi$  interactions between the electron-rich aromatic rings and the electron-deficient C<sub>60</sub> guest.



(8) (a) Georghiou, P. E.; Mized, S.; Chowdhury, S. *Tetrahedron Lett.* **1999**, *40*, 611. (b) Mized, S.; Georghiou, P. E.; Ashram, M. *J. Chem. Soc., Perkin Trans.* **2000**, *2*, 277, and references therein.

(9) Ruoff, R. S.; Tse, D. S.; Malhotra, R.; Lorents, D. C. *J. Phys. Chem.* **1993**, *97*, 3379–3383.

(10) Cheng, P.-C. Ph.D. Dissertation, Boston College, 1996.

(11) Seiders, T. J.; Baldrige, K. K.; Elliott, E. L.; Grube, G. H.; Siegel, J. S. *J. Am. Chem. Soc.* **1999**, *121*, 7439–7440.

(12) Baird, T.; Gall, J. H.; MacNicol, D. D.; Mallinson, P. R.; Michie, C. R. *J. Chem. Soc., Chem. Commun.* **1988**, 1471–1473, and references therein.

**Complexation Studies.** Supramolecular complex formation between C<sub>60</sub> and the geodesic compounds **3**, **4**, and **5b** was studied using <sup>1</sup>H NMR spectroscopy.<sup>15</sup> For the 1:1 complexation process between C<sub>60</sub> and **4** in solution (eq 4, for example), the

(13) Decachlorocorannulene was prepared by direct chlorination of corannulene: Scott, L. T. *Pure Appl. Chem.* **1996**, *68*, 291–300.

(14) Rai, A. K. M.S. Thesis, Boston College, 1997.

(15) Fielding, L. *Tetrahedron* **2000**, *56*, 6151.

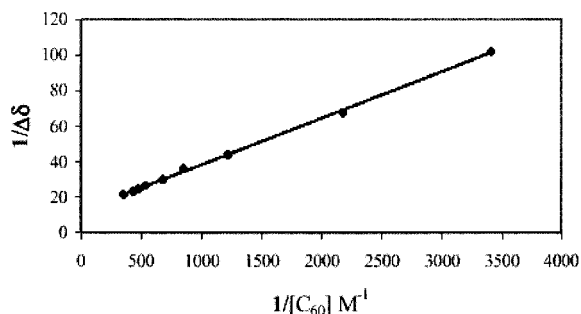


**Figure 3.** Double reciprocal (Benesi–Hildebrand) plot of  $^1\text{H}$  NMR chemical shift data for the  $\text{C}_{60}$ :**4** system in toluene- $d_8$  at 298 K.

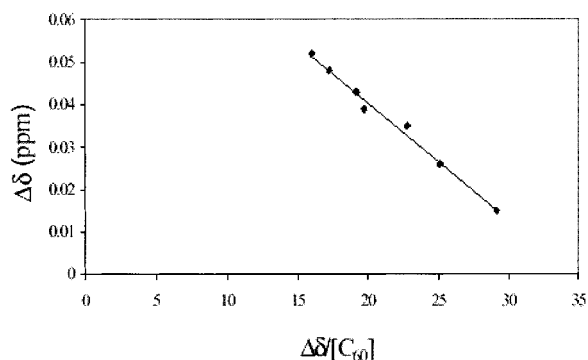


**Figure 4.**  $x$ -Reciprocal plot (Foster–Fyfe) of  $^1\text{H}$  NMR chemical shift data for the  $\text{C}_{60}$ :**4** system in toluene- $d_8$  at 298 K.

association constant  $K_{\text{assoc}}$  (eq 5) can be determined using the NMR version of the Benesi–Hildebrand treatment (Figure 3),<sup>16,17</sup> which has also been referred to as the Mathur<sup>18</sup> or Hanna–Ashbaugh<sup>19</sup> treatment.<sup>15</sup>



$$K_{\text{assoc}} = [\text{C}_{60}:\mathbf{4}]/([\text{C}_{60}] \cdot [\mathbf{4}]) \quad (5)$$

In our case, since the amounts of host materials were limited, and following the requirements for the Benesi–Hildebrand treatment, we also used the Foster–Fyfe method (eq 6),<sup>20</sup> which Fielding<sup>15</sup> has described as being more appropriate for calculating  $K_{\text{assoc}}$ . In eq 6,  $\Delta\delta$  is the change in chemical shift(s) of

$$\Delta\delta/[\text{C}_{60}] = -K_{\text{assoc}}\Delta\delta + K_{\text{assoc}}\Delta\delta_{\text{max}} \quad (6)$$

protons of the host molecule induced by the addition of  $\text{C}_{60}$ , with respect to uncomplexed host. A plot of  $\Delta\delta/[\text{C}_{60}]$  against  $\Delta\delta$  (also referred to as an  $x$ -reciprocal plot) for the complexation of  $\text{C}_{60}$  with **4** in toluene- $d_8$  is shown in Figure 4. The value of  $-K_{\text{assoc}}$  is determined from the slope, and  $\Delta\delta_{\text{max}}$  is obtained from the intercept by extrapolation of the  $x$ -reciprocal plot to infinite dilution. Table 1 lists the values of  $K_{\text{assoc}}$  at 298 K determined for  $\text{C}_{60}$  with each of host compounds **3**, **4**, and **5b** in toluene- $d_8$ .

The stoichiometry of the complex in each solution in the concentration range examined was determined to be 1:1 using a mole ratio method. Figure 5 shows the mole ratio plot for the

**Table 1.**  $K_{\text{assoc}}$  Values ( $\text{M}^{-1}$ ) for  $\text{C}_{60}$  Complexes with **3**, **4**, and **5b** in Toluene- $d_8$  at 298 K<sup>a</sup>

complex	method	run 1 ( $r^2$ )	run 2 ( $r^2$ )	average
$\text{C}_{60}$ : <b>3</b>	A	440 ± 40 (0.99)	468 ± 16 (0.99)	454 ± 30
	B	479 ± 33 (0.96)	468 ± 22 (0.99)	474 ± 28
$\text{C}_{60}$ : <b>4</b>	A	359 ± 10 (0.99)	377 ± 18 (0.99)	368 ± 15
	B	362 ± 16 (0.99)	353 ± 34 (0.96)	358 ± 27
$\text{C}_{60}$ : <b>5b</b>	A	286 ± 31 (0.99)	274 ± 25 (0.99)	280 ± 28
	B	284 ± 40 (0.85)	329 ± 37 (0.92)	306 ± 38

<sup>a</sup> Note: method A is the double reciprocal treatment (Figure 3), and method B is the  $x$ -reciprocal treatment (Figure 4);  $r^2$  is the correlation coefficient obtained from the linear regression analysis of the respective plots.

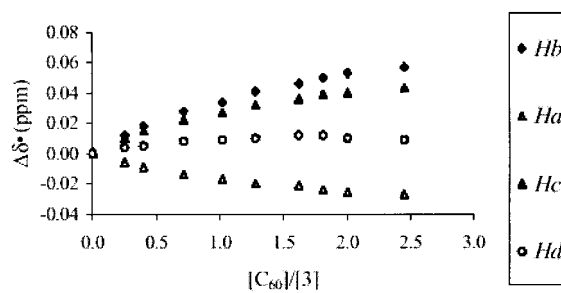


**Figure 5.** Plot of chemical shift changes ( $\Delta\delta$ ) versus mole ratio  $[\text{C}_{60}]/[\mathbf{3}]$  for protons  $\text{H}_{a-d}$  of **3** in toluene- $d_8$ .

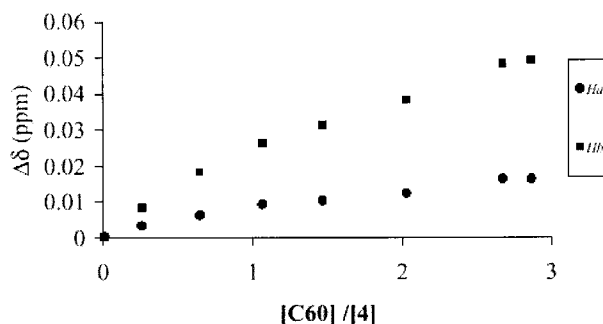


**Figure 6.** Plot of chemical shift changes ( $\Delta\delta$ ) versus mole ratio  $[\text{C}_{60}]/[\mathbf{4}]$  for protons  $\text{H}_{a-b}$  of **4** in toluene- $d_8$ .

chemical shifts of all four sets of protons in host **3**. It is evident that proton “ $\text{H}_a$ ” on the corannulene moiety is shielded by  $\text{C}_{60}$ , whereas the aromatic protons “ $\text{H}_b$ ” and “ $\text{H}_c$ ” on the aryl substituents are deshielded and exhibit somewhat larger changes in their chemical shifts. These observations are consistent with a complex in which the  $\text{C}_{60}$  guest is included deep into the cavity of **3** (Figure 2), and the relatively small changes seen in the chemical shift for the methyl protons on the more remote methoxy groups provide additional support for this view. The corresponding mole ratio plots for hosts **4** and **5b** are shown in Figures 6 and 7, respectively.

In the weaker complexes, with hosts **4** and **5b**, the protons on the corannulene moiety are less strongly affected by the  $\text{C}_{60}$ . This observation may signify that the  $\text{C}_{60}$  sits higher above the bowl in these complexes, interacting predominantly with the aryl substituents protruding from the  $\text{C}_5$ -symmetrical corannulene scaffold. In host **4**, not all of the aromatic protons are affected to the same degree by the complexed  $\text{C}_{60}$ ; only the protons on carbon 1 of the naphthalene units experience any significant deshielding. Such a localized effect suggests that these protons may be influenced by the  $\text{C}_{60}$  through relatively weak “edge-to-face” interactions<sup>21</sup> of the naphthyl groups, in contrast to the more extensive “face-to-face”  $\pi$ - $\pi$  stacking

(16) Benesi, A.; Hildebrand, J. H. *J. Am. Chem. Soc.* **1949**, *71*, 2703.

(17) Mizyed, S.; Ashram, M.; Miller, D. O.; Georghiou, P. E. *J. Chem. Soc., Perkin Trans. 2* **2001**, 1916–1919.

(18) Mathur, R.; Becker, E. D.; Bradley, R. B.; Li, N. C. *J. Phys. Chem.* **1963**, *67*, 2190.

(19) Hanna, M. W.; Ashbaugh, A. L. *J. Phys. Chem.* **1964**, *68*, 811.

(20) Forster, R.; Fyfe, C. A. *J. Chem. Soc., Chem. Commun.* **1965**, 642.

(21) Beer, P. D.; Gale, P. A.; Smith, D. K. *Supramolecular Chemistry*; Oxford University Press: New York, 1999.



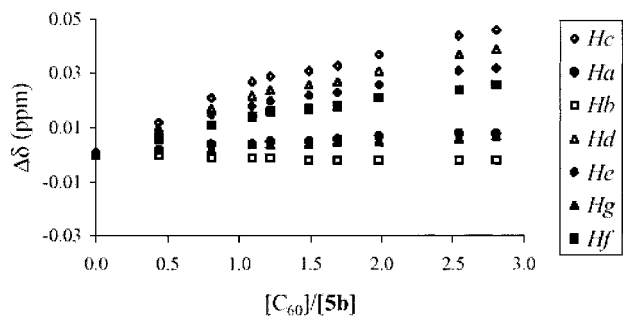


**Figure 7.** Plot of chemical shift changes ( $\Delta\delta$ ) versus mole ratio  $[C_{60}]/[5b]$  for protons  $H_{a-g}$  of **5b** in toluene- $d_8$ .

interactions possible with the smaller aryl substituents in compound **3**. From our earlier findings<sup>8</sup> on the relatively strong complexation of C<sub>60</sub> with calix[4]naphthalenes, we had expected host **4** to bind C<sub>60</sub> more strongly than the other hosts studied here (**3** and **5b**); however, steric constraints in compound **4** presumably prevent the naphthyl groups from lining up to allow good face-to-face  $\pi$ - $\pi$  stacking interactions with the  $\pi$ -system of C<sub>60</sub>.

## Conclusions

The degree of curvature on the concave face of corannulene at the van der Waals surface closely matches that on the convex face of C<sub>60</sub> at its van der Waals surface. Thus, the two ring systems are geometrically well suited to make good face-to-face contact. Furthermore, these two  $\pi$ -surfaces are electronically complementary, the concave face of corannulene being electron rich and the convex face of C<sub>60</sub> being electron deficient, according to density functional calculations. Electron-rich arms on the corannulene capable of embracing C<sub>60</sub> in the donor-acceptor complex would be expected to enhance the attractive noncovalent interactions between these partners. The 1:1 complexes between C<sub>60</sub> and the corannulene thioethers **3**, **4**, and **5b** described here constitute the first reported examples of complex formation between geodesic polyarene derivatives and another curved  $\pi$ -surface. Comparisons of the NMR data for these three complexes indicate that the C<sub>60</sub> interacts most strongly with the corannulene moiety in host **3**.

## Experimental Section

**1,3,5,7,9-Pentachlorocorannulene (2).** A 200 mg (0.8 mmol) sample of corannulene was added to 10.0 mL (10.0 mmol) of a 1.0 M solution of iodine monochloride (ICI) in methylene chloride at room temperature, and the resulting purple suspension was stirred at room temperature for 48 h. The reaction mixture was then washed with 5% aqueous sodium thiosulfate (2 × 50 mL), 10% hydrochloric acid (2 × 50 mL), and saturated brine (2 × 50 mL) to give a yellow suspension of the crude product in methylene chloride. The solvent was removed under reduced pressure, and the resulting yellow solid was thoroughly digested in 50 mL of hexane. The hexane was carefully removed with a Pasteur pipet, and the process was repeated several times, first with hexane and then with methylene chloride to leave a pale yellow solid. The material thus obtained consisted predominantly of 1,3,5,7,9-pentachlorocorannulene (**2**), contaminated by small amounts of the symmetrical tetrachlorocorannulene **5a**, two unsymmetrical tetrachlorocorannulenes (**5b** and **5c**), and some hexachlorocorannulenes. Recrystallization from diphenyl ether gave 135 mg (40%) of pure 1,3,5,7,9-pentachlorocorannulene as a pale yellow solid: mp 432–434 °C; <sup>1</sup>H NMR (400 MHz, C<sub>6</sub>D<sub>6</sub>/CS<sub>2</sub>)  $\delta$  7.99 (s, 5H); <sup>13</sup>C NMR (100 MHz, DMSO- $d_6$ , 100 °C) too insoluble to give signals. HRMS: Calcd for C<sub>20</sub>H<sub>5</sub>Cl<sub>5</sub> (M<sup>+</sup>), 419.9833. Found: 419.9836.

**General Procedure for Preparation of Sodium Thiolates (RSNa).** Under a nitrogen atmosphere, 230 mg (0.01 mol) of sodium metal was

dissolved in anhydrous ethyl alcohol (1.0 mL) at room temperature over a period of 30 min. The thiol (0.01 mol) was then added slowly, and the resulting solution was stirred for another 1 h at room temperature. Evaporation of the solvent under reduced pressure gave a solid that was washed several times with ethyl ether, isolated by filtration, and dried under vacuum to give the desired sodium thiolate as a colorless solid (store under nitrogen).

**1,3,5,7,9-Pentakis(4-methoxyphenylthio)corannulene (3).** 1,3,5,7,9-Pentachlorocorannulene (100 mg, 0.237 mmol) and sodium 4-methoxybenzene thiolate (385 mg, 2.37 mmol), prepared as above from 4-methoxythiophenol, were stirred in 10 mL of 1,3-dimethylimidazolidin-2-one (DMEU) at room temperature under nitrogen for 48 h. The deep yellow solution was then added to toluene (50 mL), washed with water (3 × 100 mL) and saturated NaCl solution, dried over MgSO<sub>4</sub>, and concentrated to dryness under reduced pressure. The yellow residue was chromatographed on silica gel using diethyl ether/petroleum ether (1:1) as eluent to afford 110 mg (50%) of 1,3,5,7,9-pentakis(4-methoxyphenylthio)corannulene as a yellow solid: mp 180 °C dec; <sup>1</sup>H NMR (300 MHz, CDCl<sub>3</sub>)  $\delta$  7.66 (s, 5H), 7.30 (d,  $J$  = 9.0 Hz, 10H), 6.84 (d,  $J$  = 9.0 Hz, 10H), 3.84 (s, 15H); <sup>13</sup>C NMR (75 MHz, CDCl<sub>3</sub>)  $\delta$  160.25, 138.10, 135.83, 134.86, 131.76, 126.66, 125.38, 115.76, 56.07. HRMS: Calcd for C<sub>55</sub>H<sub>40</sub>S<sub>5</sub>O<sub>5</sub> (M<sup>+</sup>), 940.1479. Found: 940.1479.

**1,3,5,7,9-Pentakis(2-naphthylthio)corannulene (4).** 1,3,5,7,9-Pentachlorocorannulene (100 mg, 0.237 mmol) and sodium 2-naphthylthiolate (431 mg, 2.37 mmol), prepared as above from 2-naphthalenethiol, were stirred in 10 mL of 1,3-dimethylimidazolidin-2-one (DMEU) at room temperature under nitrogen for 48 h. The deep yellow solution was then added to toluene (50 mL), washed with water (3 × 100 mL) and saturated NaCl solution, dried over MgSO<sub>4</sub>, and concentrated to dryness under reduced pressure. The yellow residue was chromatographed on silica gel using diethyl ether/petroleum ether (1:9) as eluent to afford 135 mg (55%) of 1,3,5,7,9-pentakis(2-naphthylthio)corannulene as a yellow solid: mp 172–174 °C; <sup>1</sup>H NMR (500 MHz, CDCl<sub>3</sub>)  $\delta$  7.94 (s, 5H), 7.78 (d,  $J$  = 8.0 Hz, 5H), 7.77 (s, 5H), 7.59 (d,  $J$  = 7.5 Hz, 5H), 7.53–7.49 (m, 15H), 7.25 (d,  $J$  = 8.5 Hz, 5H); <sup>1</sup>H NMR (500 MHz, toluene- $d_8$ )  $\delta$  8.16 (s, 5H), 7.62 (s, 5H), 7.41 (d,  $J$  = 7.5 Hz, 5H), 7.16–7.11 (m, 25H). HRMS (APCI): Calcd for C<sub>70</sub>H<sub>41</sub>S<sub>5</sub> (M<sup>+</sup>+1), 1041.1810. Found: 1041.1765.

**1,3,6,8-Tetrakis(4-methoxyphenylthio)corannulene (5b).** When the above synthesis of 1,3,5,7,9-pentakis(4-methoxyphenylthio)corannulene (**3**) is performed using pentachlorocorannulene that is still contaminated with tetrachlorocorannulenes, the three tetrakis(4-methoxyphenylthio)corannulenes (**5b**, **6b**, and **7b**) are formed as byproducts. Column chromatography on silica gel using diethyl ether/petroleum ether (1:1) as eluent gives a mixture of the two unsymmetrical tetrakis(4-methoxyphenylthio)corannulenes (**6b** and **7b**) in the fastest moving band, and the second fraction contains 1,3,5,7,9-pentakis(4-methoxyphenylthio)corannulene (**3**). The third band contains 1,3,6,8-tetrakis(4-methoxyphenylthio)corannulene (**5b**): <sup>1</sup>H NMR (400 MHz, CDCl<sub>3</sub>)  $\delta$  7.93 (s, 2H), 7.71 (s, 2H), 7.43 (d,  $J$  = 8.8 Hz, 4H), 7.40 (s, 2H), 7.32 (d,  $J$  = 8.8 Hz, 4H), 6.90 (d,  $J$  = 8.8 Hz, 4H), 6.85 (d,  $J$  = 8.8 Hz, 4H), 3.84 (s, 6H), 3.82 (s, 6H); <sup>13</sup>C NMR (100 MHz, CDCl<sub>3</sub>)  $\delta$  159.82, 159.64, 137.79, 136.56, 136.21, 135.47, 134.30, 134.17, 133.99, 131.60, 131.34, 130.80, 127.78, 126.65, 126.42, 125.61, 125.17, 115.37, 115.25, 55.60, 55.57. HRMS: Calcd for C<sub>48</sub>H<sub>34</sub>S<sub>4</sub>O<sub>4</sub> (M<sup>+</sup>), 802.1340. Found: 802.1340.

**Complexation Measurements.** C<sub>60</sub> (99.5%) was purchased from Sigma-Aldrich. All <sup>1</sup>H NMR spectra were recorded at 298 K on a Bruker Avance Instrument at 500 MHz, using a 16K data table for a 10.0 ppm sweep width having a digital resolution of 0.321 Hz. The solvent was toluene- $d_8$  (99.6%) purchased from Cambridge Isotope Laboratories, Inc. Mass determinations were performed on a CAHN-27 electromicrobalance capable of mass determinations to 5 × 10<sup>-6</sup> g. To obtain the association constants  $K_{\text{assoc}}$  corresponding to complex formation, changes in the chemical shifts ( $\Delta\delta$ ) as a function of  $[C_{60}]$  were determined. Approximately 1.000 mg amounts of the host compound (**3**, **4**, or **5b**) were dissolved in 1.00 mL of toluene- $d_8$  in an NMR tube, to which were added portions of C<sub>60</sub> (approximately 0.100 mg amounts). After sonication for 15 min to dissolve all of the C<sub>60</sub>, the NMR data were collected. At least 8–10 data points were collected for each run, and each run was conducted in duplicate. The changes in

chemical shifts ( $\Delta\delta$ ) were plotted against  $[C_{60}]$  for each run, and the resulting mole ratio plots (see Figures 5–7) level off at around a 1:1 ratio of  $C_{60}$  and **3**, **4**, or **5b**, indicating the formation of a 1:1 complex in each case. To calculate  $K_{\text{assoc}}$  values, the slopes and the intercepts obtained from linear regression analyses of both the Benesi–Hildebrand “linear double reciprocal” plot and the Foster–Fyfe “ $x$ -reciprocal” plot method were used (Figures 3 and 4, respectively). The correlation coefficients obtained from the Benesi–Hildebrand plots were slightly superior to those obtained with the Foster–Fyfe plots (Table 1). The uncertainties in  $K_{\text{assoc}}$  values were calculated from the uncertainties in

the slopes and intercepts of these plots, which were obtained from nonlinear regression analysis using Sigmaplot v3.0.

**Acknowledgment.** We thank the National Science Foundation, the Natural Sciences and Engineering Research Council of Canada (NSERC), and the Memorial University of Newfoundland for financial support of this work and Dr. J. Banoub, Fisheries and Oceans, Canada, Special Projects, St. John’s, Newfoundland, Canada, for the APCI-MS of compound **4**.

JA016761Z